# Impacts of Climate Change on Subsurface Water Environment in the Lower Seyhan River Basin

## －Final Results of Calibration and Projection－

**Katsuyuki FUJINAWA[1] Takahiro IBA[1] and Yoichi FUJIHARA[2]**

[1]*Geo-environmental engineering, Faculty of engineering, Shinshu University*
*550 Wakasato, Nagano, Nagano 380-8533, JAPAN*
[2]*Research Institute for Humanity and Nature*

## 1. Introduction

According to IPCC, climate change is expected to cause abnormal weather and sea-level rise, and may accordingly influence water-resources management for agricultural productions. Although groundwater may be considered to be an important water resource as an substitute of reducing surface water resources, subsurface water environment can also be significantly affected by climatic, hydrogeologic and anthropogenic conditions in a very complicated way. The objective of this study is to assess future subsurface water environment of the arid area extending in the Seyhan River Delta, the Cukurova plain, Turkey, in accordance with climate change and agricultural activities.

Major phenomena related to the subject include flow and salinity of groundwater in coastal aquifers, salinity in lagoons, and salt accumulation on land surfaces. Quantitative assessment of impacts on such complicated phenomena can only be performed by using numerical models. To achieve this objective, a coupled, 2-D, groundwater flow and mass transport model, SIFEC (Salt-water Intrusion by Finite Elements and Characteristics), was developed and applied to assess future changes under various scenarios. SIFEC is a numerical model based on a coupling of the Galerkin-finite element method for saturated-unsaturated, density-dependent flow and the method of characteristics for mass transport. Basic methodology, properties, accuracy, etc, have been described elsewhere[1)] and will not be repeated here.

## 2. Scenarios

Provided with temporal changes in sea level, evapo-transpiration, precipitation, irrigation practice, groundwater use, and base flow from mountainous area into lowland aquifers of the lower Seyhan river basin (LSRB), a specific version of SIFEC was applied to assess impacts of climate change and enhanced abstraction on groundwater table, salinity distribution in groundwater including seawater intrusion, water logging, salt accumulation on land surface, salinity concentration in lagoon water for various scenarios.

Simulation models were run under several scenarios. Each scenario is composed of five elements as shown in **Fig.1**; that is, sea level rise, climate, recharge due to irrigation, abstraction rate, and inland B.C.

Each element has three to four components. The sea-level-rise(S) has three components; that is, 0.0 cm rise by 2100 (denoted by Sc), 0.88 cm rise by 2100 (Maximum rise projected with SRES A1Fl scenario and reported in the IPCC 3rd AR

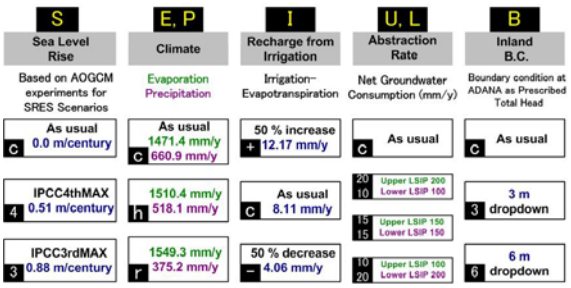


Fig.1 Scenarios for Projecting Subsurface Environment in 2070

**Table 1**. Rainfall and Evaporation

| | Rainfall (mm/y) | Rainfall (m/d) | Evaporation (mm/y) | Evaporation (m/d) |
|---|---|---|---|---|
| Current | 660.9 | 0.00181 | 1471.4 | 0.00403 |
| 2070 by MRI | 379.2 | 0.00104 | 1522.2 | 0.00417 |
| 2070 by CCSR | 371.1 | 0.00104 | 1576.4 | 0.00432 |
| 2070 Mean of MRI and CCSR | 375.2 | 0.00103 | 1549.3 | 0.00424 |

**Table 2** Abstraction Rate of Representative Wells

| | Abstraction ($m^3$/day) | | | | | |
|---|---|---|---|---|---|---|
| | Well 1 | Well 2 | Well 3 | Well 4 | Well 5 | Well 6 |
| Pre-Irrigation | 0.00 | 0.00 | 0.00 | 0.00 | 0.00 | 0.00 |
| Current | 0.03 | 0.22 | 0.92 | 0.44 | 0.09 | 0.03 |
| U20L10 | 5.31 | 3.82 | 1.85 | 1.67 | 0.81 | 0.00 |
| U15L15 | 3.98 | 2.87 | 2.78 | 2.51 | 1.22 | 0.00 |
| U10L20 | 2.65 | 1.91 | 3.70 | 3.35 | 1.62 | 0.00 |

denoted by S3), and 0.51 cm rise by 2100 (Maximum rise projected with SRES A2 scenario and reported in the IPCC 4th AR, denoted by S4).

Evaporation rates from water surfaces in the climate element (E) were evaluated with the aid of the Penman method using the temperature projected by MRI-RCM ( Meteorological Research Institute – Regional Climate Model) and CCSR-RCM (Center for Climate System Research, University of Tokyo) and has three components; that is, 1471.4 mm/y (currently observed and denoted by Ec), 1549.3 mm/y in 2070 (mean of MRI and CCSR Projection for SRES (Special Report on Emission Scenario) A2 scenario and denoted by Er), and 1510.4 mm/y in 2070 (mean of the currently observed and the mean of MRI and CCSR Projection, denoted by Eh).

Precipitation rate in the climate element (P) has three components; that is, 660.9 mm/y (currently observed and denoted by Pc), 375.2 mm/y in 2070 (mean of MRI and CCSR projection for SRES A2 scenario and denoted by Pr), and 518.1 mm/y in 2070 (mean of the currently observed and the mean of MRI and CCSR Projection and denoted by Ph). Table 1 shows the adopted values of precipitation and Evaporation.

The recharge-from-irrigation element has three components; that is, 8.11 mm/y (calibrated current estimation and denoted by Ic), 12.17 mm/y in 2070 (50 % increase of the calibrated current estimation and denoted by I+), and 4.06 mm/y in 2070 (50 % decrease of the calibrated current estimation and denoted by I-).

The abstraction-rate element has four components; that is, as usual (calibrated current estimation and denoted by c), upper LSIP 200 and lower LSIP 100 (denoted by U20 and L10), upper LSIP 150 and lower LSIP 150 (denoted by U15 and L15), and upper LSIP 100 and lower LSIP 200 (denoted by U10 and L20). The numbers 200, 150, and 100 denote adapted future water requirements for agriculture in mm/year for the Lower Seyhan Irrigation Project and these data are converted to abstraction rates for six representative wells).

Inland boundary condition (B) in the inland B.C. element is given as a prescribed head boundary and has three components; that is, as usual (currently observed 19m above sea level at Adana city and denoted by Bc), 3 m dropdown (denoted by B3), and 6 m dropdown (denoted by B6)

Hereafter, each scenario is entitled with abbreviations used in Fig.1 such as ScEhPhI-U20L10B6, etc.

## 3. Calibration of mathematical model

(1) Calibration for pre-irrigation stage

Numerical simulations conducted so far for real fields by many researchers have usually been hampered by the lack of important data needed for calibration processes. This was also the case for this study.

Although there has been no estimation for the amount of annual groundwater recharge due to precipitation in the study area, W.Scheumann[2] describes in her book as follows;

“In the 1960s, prior to the installation of the irrigation project, rainfed agriculture was practiced on 95 % of the projected land” “The groundwater level is high, reaching a maximum level of 0.5 to 1.0 meter below land surface and a minimum of 2 to 4 meters. Large areas become water logged during the winter.”

For this pre-irrigation stage back to 1960s, it can be assumed that there were neither artificial groundwater recharge due to irrigation nor

groundwater abstraction.

Thus, natural recharge due to precipitation was applied on the entire land surface and its rate was inversely estimated so that most of the land surface becomes seepage face.

An inversion process of this simulation for the pre-irrigation stage resulted in the annual recharge rate from precipitation of 8.11mm/year. The upper

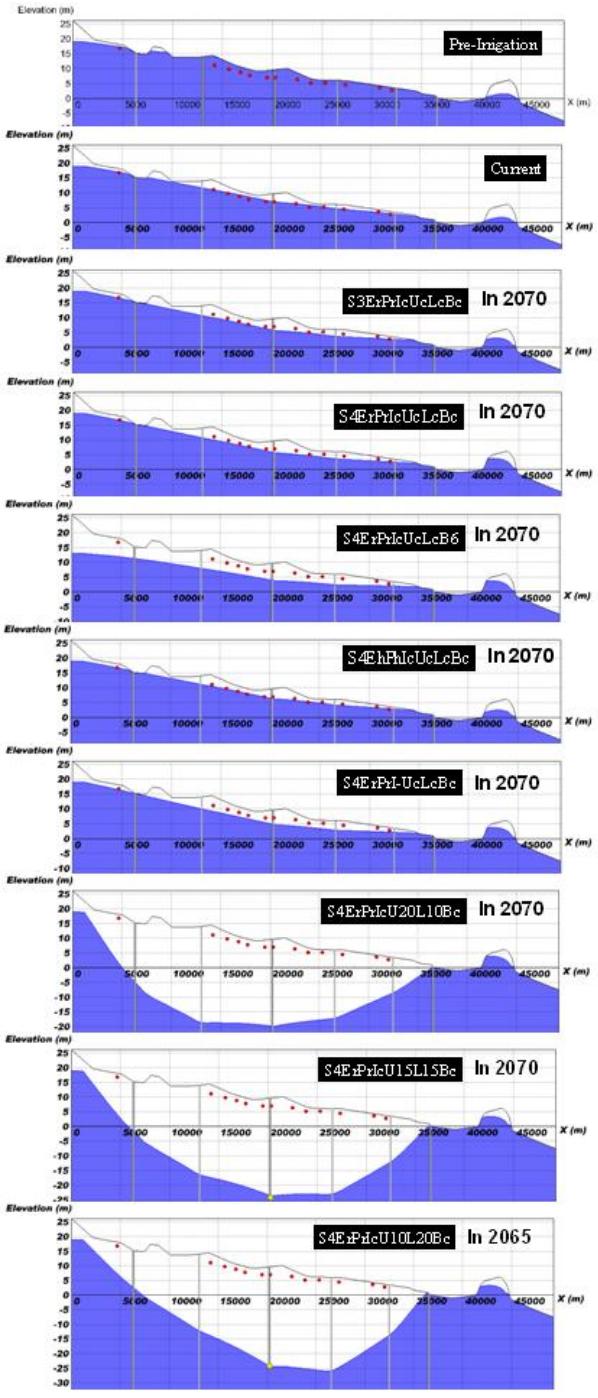


Fig.2 Groundwater tables calibrated for pre-irrigation and current stages and projected for various scenarios

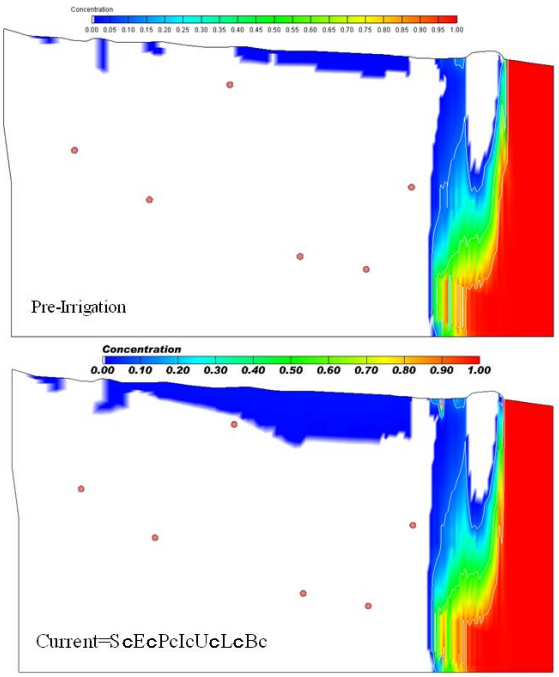


Fig.3 Distribution of groundwater salinity relative to the Mediterranean at the pre-irrigation and the current stage

most figure of **Fig.2** shows the location of the calibrated groundwater table for the pre-irrigation stage, where red dots indicate locations of observed groundwater table heights at the current stage. As Scheumann described, the land surface corresponds to the seepage face over the large area.

Water of Akyatan Lagoon was observed to have salinity of 6.8 S/m, which is higher than 5.8 S/m of the Mediterranean. In shallow zone of LSRB and in the left side of the lagoon, salinity of groundwater was also observed to be more than 0.02 S/m and less than 0.12 S/m. The upper figure of **Fig.3** shows the calculated distribution of salinity relative to the Mediterranean in the groundwater at the pre-irrigation and the current stage.

It should be noted that fresh groundwater is found in sand dune aquifer close to the Mediterranean, forming a fresh water lens above the saline groundwater, while salt water intrudes into the coastal aquifer from the sea, followed by upward flow of groundwater toward the lagoon.

**Fig.4** shows calculated distribution of groundwater vectors near the lagoon. It can be seen that in the pre-irrigation stage, groundwater used to flow upward toward land surface and the lagoon.

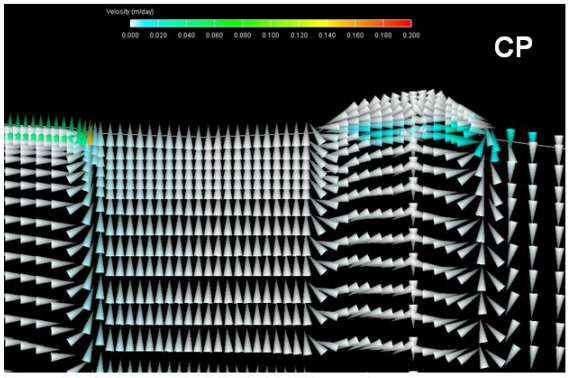


Fig.4 Groundwater Velocity at the pre-irrigation stage

(2) Calibration for the current stage

Groundwater abstraction rates of six wells were identified so that calculated groundwater table heights coincide with those by observation. Groundwater recharge rate due to irrigation in agricultural area was assumed to be the same as natural recharge rate due to precipitation for the current stage since the contribution of irrigation to groundwater-table rise is almost the same as that of precipitation.

The second figure from the top of **Fig.2** shows that the simulated groundwater table coincides quite well with the observed one. Identified values of current abstraction rate of wells are shown in Table 2.

The lower figure of **Fig.3** shows the calculated distribution of groundwater salinity at the current stage. Due to abstraction from wells, groundwater table declines compared to the pre-irrigation stage shown in Fig.2. Thus, the salinity in shallow groundwater slightly increases in agricultural areas eventually.

## 4. Influence of Evaporation from the Lagoon

Observed electric conductivity of Akyatan lagoon was 6.8 S/m, which is higher than that of the Mediterranean by 1.0 S/m due to evaporation from the lagoon. **Fig.5** is a schematic diagram illustrating input/output relations for volume and mass balance of the lagoon water. Equations for the volume and the mass balance are also shown in the figure.

Water level of the lagoon has been maintained to be the same as the Mediterranean since both water bodies are connected via a narrow channel. Condensation of salt in the lagoon water is taking place due to seepage of saline groundwater, inflow of sea water, and evaporation.

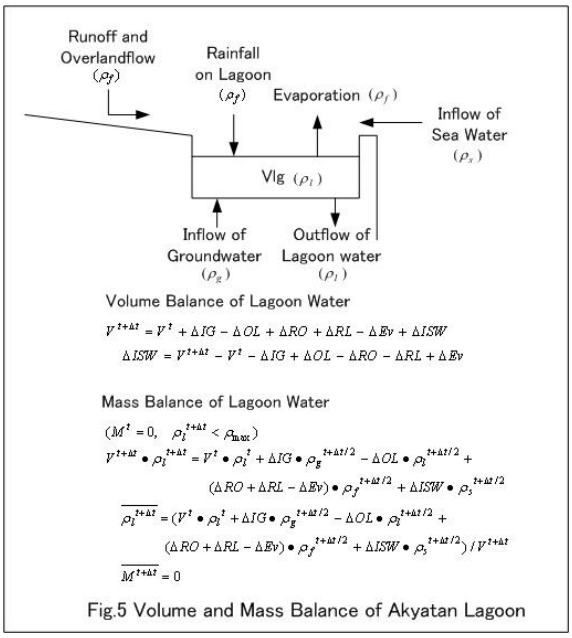


Fig.5 Volume and Mass Balance of Akyatan Lagoon

Unknown volume of sea water inflow to the lagoon during a simulation time span of $\Delta t$, $\Delta ISW$, can be calculated by the second equation describing the volume balance of the lagoon water. Another unknown factor $\Delta RO$, the amount of runoff and overland flow during $\Delta t$, is identified so that salinity of the lagoon water is constant. Unknown variable $\rho_l^{t+\Delta t}$, density of the lagoon water at $t+\Delta t$, can be calculated by the second equation for the mass balance of the lagoon water. $\Delta IG$ (inflow of groundwater) and $\Delta OL$ (outflow of lagoon water) as well as $\rho_g$ (density of groundwater) and $\rho_l$ ( density of lagoon water) can also be evaluated in the calculation process of simulation runs.

**Table 1** shows the current and the projected rate of rainfall and evaporation in2070. The current evaporation and the precipitation rate are 1471.1 mm/year and 660.9 mm/year, respectively, while average values of future evaporation and rainfall rate projected for 2070 by using MRI and CCSR are 1549.3 mm/year and 375.2 mm/year, respectively. The difference between the evaporation and the precipitation rate enormously widens from 810.5 mm/year to 1174.1 mm/year during the coming 70 years. Since the current maximum depth of the lagoon is less than 1 meter, condensation process is considered to be extremely significant.

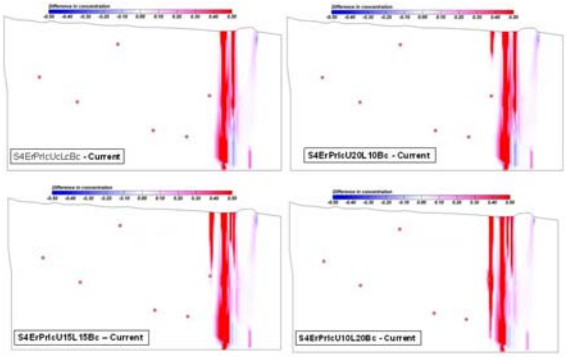


Fig.6 Difference in Groundwater Salinity between Runs of Current and Each Scenario with different Abstraction rates

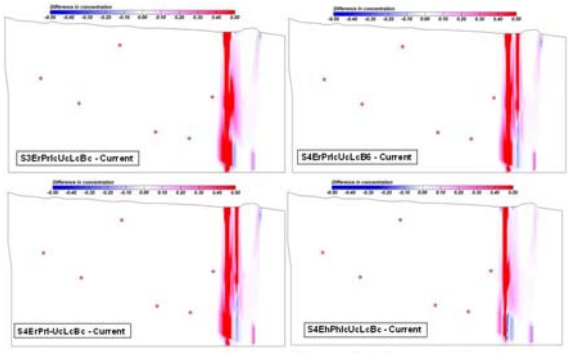


Fig.7 Difference in Groundwater Salinity between Runs of Current and Each Scenario with Different Components

## 5. Changes in groundwater table

According to the result of S3ErPrIcUcLcBc run, sea level rise of 0.88 m/century, increase in evaporation, and decrease in precipitation cause a slight decline of groundwater table. A build-up effect of groundwater table in the sand dune aquifer can be attributed to high salinity of groundwater beneath the lagoon and shrinkage of fresh water lens in the aquifer.

S4ErPrIcUcLcBc scenario is different from S3ErPrIcUcLcBc only in that projected sea-level rise of S4 is 0.37 m/century smaller than that of S3. The third and fourth projected results from the top of Fig.2 show that the amount of sea level rise will not affect much to groundwater table

S4ErPrIcUcLcB6 run indicates that decline of boundary head will cause significant dropdown of groundwater table.

According to the result of S4EhPhIcUcLcBc run, little increase in evaporation and little decrease in precipitation will not affect much on groundwater table. However, as shown in the fourth figure from the bottom of Fig.2 reduction of recharge from irrigation may cause groundwater table dropdown to some extent.

Enhanced groundwater abstraction can cause significant dropdown of groundwater table as shown in the last three figures of Fig.2. The shape of groundwater table and the degree of its dropdown depend largely on the amount of abstraction rates and its distribution.

## 6. Changes in groundwater salinity

In Figs. 6 and 7, changes in groundwater salinity for several scenarios are illustrated in terms of difference of concentration relative to the Mediterranean between the result of scenario runs and the current distribution shown in the lowest figure of Fig.3. These figures show finger-like, complicated distribution of salinized zone in groundwater beneath the lagoon. This can be attributed to the following factors. First, the width of the lagoon is currently 4,552m and will expand to 4,928 m in 2070. Second, the depth of the lagoon is less than 1 m and the bottom of the lagoon is relatively flat. Third, the lagoon is discharged in a complicated way by horizontal groundwater flow from inland and sand dune together with upward groundwater flow via an deeper aquifer of higher permeability.

groundwater flow via an deeper aquifer of higher permeability.

Impacts of abstraction on groundwater salinity are shown in Fig.6. Although the distribution and the rate of abstraction for scenario S4ErPrIcUcLcBc are the same as the current condition, high salinity zone in groundwater deeply penetrates beneath the lagoon. This is mostly attributed to condensation of salt in the lagoon water due to increased evaporation and decreased precipitation.

According as the abstraction rates increase near the lagoon, saline water in the lagoon infiltrates more into the aquifer and makes saline zone in groundwater beneath the lagoon deeper.

Higher sea level rise, as depicted by S3ErPrIcUcLcBc in Fig.7, may cause slightly larger salt-water intrusion compared to the result of S4ErPrIcUcLcBc of Fig.6. The impact of lowered inland boundary head and reduced recharge from irrigation on the formation of saline zone in groundwater does not seem to be recognizable.

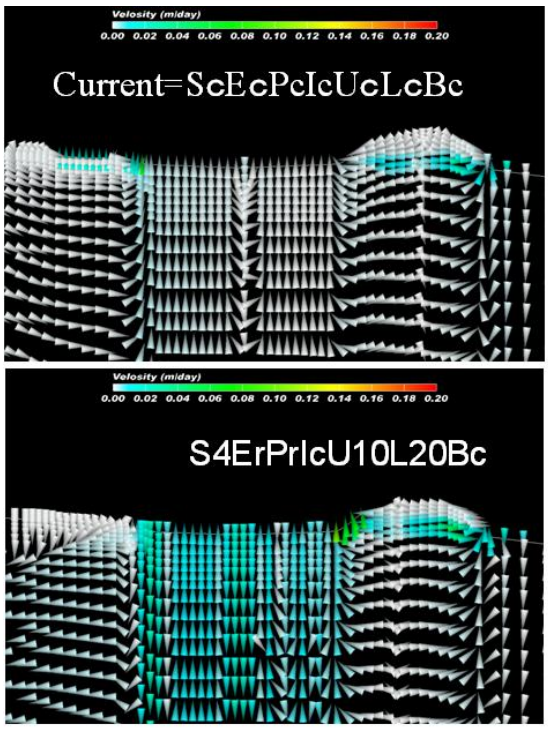


Fig.8 Distribution of Groundwater Flow Vectors

However, reduced evaporation and increased precipitation for S4EhPhIcUcLcBc compared to S4ErPrIcUcLcBc obviously reduces saline groundwater zone as shown in the bottom right figure of Fig.7.

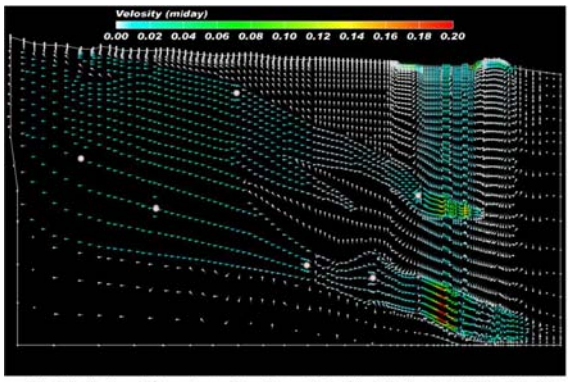


Fig.9 Distribution of Groundwater Flow Vectors in the Whole Region for S4ErPrIcUcLcB6

## 7. Groundwater velocity distribution

Fig.8 shows calculated groundwater flow vectors near the lagoon for the current stage and S4ErPrIcU10L20Bc. Due to high water table during the pre-irrigation stage, Groundwater discharges into the lagoon and there is no infiltration from the lagoon as shown in Fig.4. At the current stage, however, a slight downward vector can be seen near the center of the lagoon, which is attributed to the decline of water table from the pre-irrigation stage due to groundwater abstraction.

The result of S4ErPrIcU10L20Bc run exhibits more complicated flow pattern due to the significant decline of water table accompanied by enhanced abstraction. Discharge of fresh water into the lagoon from fresh-water lens of the dune aquifer is also enhanced.

Fig.9 shows groundwater velocity vectors in the whole analytical domain. The greatest velocity is seen in the lowest part of the aquifer beneath the lagoon. It can also be observed that fresh groundwater supplied along the mountainous boundary flows mostly in the high permeable zone toward the Mediterranean and flows upward beneath the lagoon.

## 8. Salinity of the lagoon

Salinity of the lagoon can be affected by evaporation, precipitation, run-off and overland flow, sea-water inflow, and groundwater discharge and recharge. As mentioned before, the amount of run-off and overland flow is unknown. Therefore, a factor ROF, defined by $(\Delta RO + \Delta RL) / \Delta RL$, was inversely identified so that the simulated salinity of the lagoon remains constant for a certain period of time. The identified ROF is 2.1404.

Fig.10 shows temporal changes in the salinity of the lagoon. Small change in ROF can affect the salinity as shown by the result of ScErPrIcUcLcBc-2.000, where ROF is 2.000. Reduced evaporation and increased precipitation of S4EhPhIcUcLcBc can speed down the accumulation of salt in the lagoon compared to S4ErPrIcUcLcBc. Salt accumulation in the lagoon can be delayed by sea level rise as shown by the result for S3ErPrIcUcLcBc, but eventually reaches to a higher salinity level compared to S4ErPrIcUcLcBc.

## 9. Salt accumulation on land

The amount of salt accumulated on land surface for scenarios S4ErPrIcUcLcBc and S4ErPrIcU20L10Bc is shown in Fig.11. In the low-lying area near the lagoon where groundwater seeps out, discharging groundwater transports

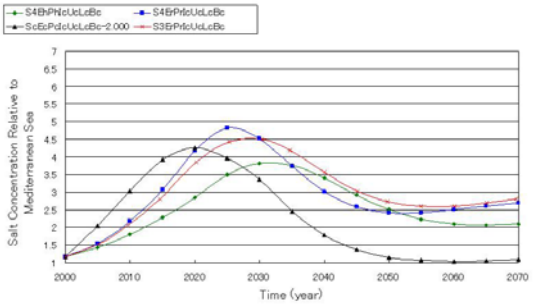


Fig.10 Temporal Changes in the Salinity of the Lagoon

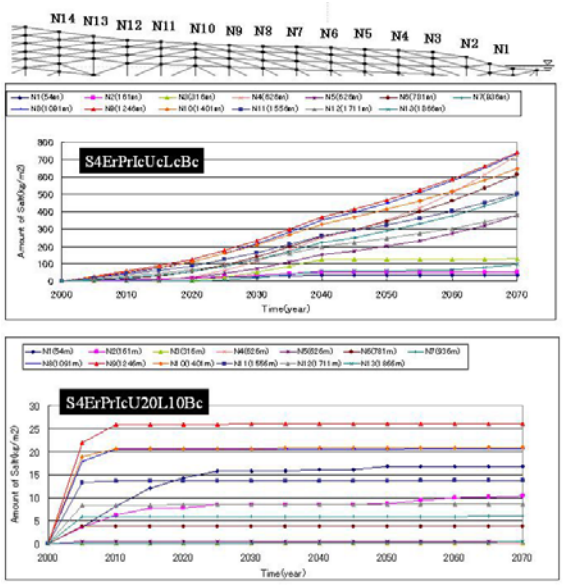


Fig.11 Accumulated Salt of Land Surface

salt on land surface and salt accumulates there due to evaporation. Since the mechanism for the accumulated salt to be carried away by overland flow or drainage into open channels has not been taken into consideration in the conceptual model, the salt transported by groundwater onto land surface remains there.

The maximum amount of the accumulated salt reaches more than 700 kg/m$^2$ for S4ErPrIcUcLcBc after 70 years time span since most of the low-lying area near the lagoon remains to be a seepage face, while, for S4ErPrIcU20L10Bc, accumulation of salt on land surface stops after a certain period of time due to dropdown of the water table caused by abstraction. The simulated amount of the accumulated salt has to be carefully evaluated. It should be noted that there are uncertainty in input data of initial salinity distribution in groundwater together with boundary conditions of prescribed flux and its salinity, which should be provided along land surface. To ensure the accuracy of projected results, input data should be based on a detailed field studies.

## 10. Summary

Followed by two-steps calibration processes, projections for assessing impacts of climate change on subsurface water environment of LSRB were performed for various scenarios based on sea-level rise, climatic elements, irrigation practice, river run-off, and groundwater abstraction. Outputs of the projections were explained in terms of salinity of Akyatan lagoon and groundwater, groundwater table and velocity, and accumulation of salt on lands. The results can be summarized as follows;

Combination of sea-level rise, increasing evaporation, and reducing precipitation can cause significant increase in salinity in the lagoon.

Increased salinity in the lagoon in turn deteriorates groundwater quality. Salinity of groundwater can also drastically increase beneath the lagoon.

Build-up of high-saline zone in the aquifer beneath the lagoon can impede fresh groundwater flow and can cause water logging on land surface.

Water logging and increased salinity in shallow groundwater can cause severe accumulation of salt on land surface. All of increasing evaporation, sea-revel rise, and increasing groundwater abstraction contribute for the salt accumulation on land. Thus, drainage practice is strongly recommended in the future to minimize impacts of salt accumulation on land surface.

Groundwater table can decline to the level 25 m below sea level in accordance with enhanced groundwater abstraction.

## 11. References

(1) K. Fujinawa, K. Masuoka, T. Nagano, T. Watanabe, (2004): Numerical simulation modeling for salt-water intrusion in predicting impacts of sea-level rise on areas below sea-level, *Journal of Environmental Systems and Engineering, Japan Society of Civil Engineers*, No.790/VII-35,pp.35-48.

(2) W.Wcheumann, (1997): Managing Salinization-Institutional analysis of public irrigation systems, Springer-verlag, p.274.